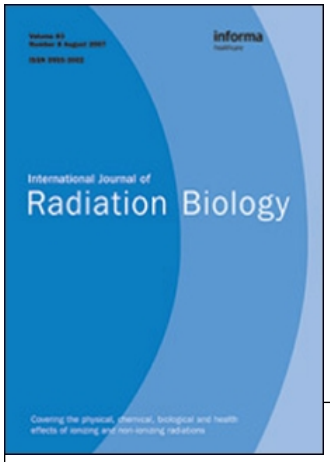

International Journal of Radiation Biology
Publication details, including instructions for authors and subscription information:
http://www.informaworld.com/smpp/title~content=t713697337

Chromosome breakpoint distribution of damage induced in peripheral blood lymphocytes by densely ionizing radiation

R. M. Anderson [a]; N. D. Sumption [a]; D. G. Papworth [a]; D. T. Goodhead [a]
[a] MRC Radiation and Genome Stability Unit, Didcot, Oxfordshire, UK

Online Publication Date: 01 January 2006

To cite this Article: Anderson, R. M., Sumption, N. D., Papworth, D. G. and Goodhead, D. T. (2006) 'Chromosome breakpoint distribution of damage induced in peripheral blood lymphocytes by densely ionizing radiation', International Journal of Radiation Biology, 82:1, 49 — 58

To link to this article: DOI: 10.1080/09553000600579231
URL: http://dx.doi.org/10.1080/09553000600579231

Int. J. Radiat. Biol., Vol. 82, No. 1, January 2006, pp. 49 – 58

Chromosome breakpoint distribution of damage induced in peripheral blood lymphocytes by densely ionizing radiation

R. M. ANDERSON, N. D. SUMPTION, D. G. PAPWORTH & D. T. GOODHEAD

MRC Radiation and Genome Stability Unit, Harwell, Didcot, Oxfordshire, UK

(Received 26 January 2005; accepted 15 January 2006)

Abstract

Purpose: To assess the chromosomal breakpoint distribution in human peripheral blood lymphocytes (PBL) after exposure to a low dose of high linear energy transfer (LET) α-particles using the technique of multiplex fluorescence *in situ* hybridization (m-FISH).

Materials and methods: Separated PBL were exposed in G_0 to 0.5 Gy ^{238}Pu α-particles, stimulated to divide and harvested ~48 – 50 hours after exposure. Metaphase cells were assayed by m-FISH and chromosome breaks identified. The observed distribution of breaks were then compared with expected distributions of breaks, calculated on the assumption that the distribution of breaks is random with regard to either chromosome volume or chromosome surface area.

Results: More breaks than expected were observed on chromosomes 2 and 11, however no particular region of either chromosome was identified as significantly contributing to this over-representation. The identification of hot or cold chromosome regions (pter,p,cen,q,qter) varied depending on whether the data were compared according to chromosome volume or surface area.

Conclusions: A deviation from randomness in chromosome breakpoint distribution was observed, and this was greatest when data were compared according to the relative surface area of each individual chromosome (or region). The identification of breaks by m-FISH (i.e., more efficient observation of interchanges than intrachanges) and importance of territorial boundaries on interchange formation are thought to contribute to these differences. The significance of the observed non-random distribution of breaks on chromosomes 2 and 11 in relation to chromatin organization is unclear.

Keywords: *High-LET α-particles, m-FISH, chromosome break, distribution*

Introduction

A number of factors are expected to confer a non-random distribution of initial radiation-induced damages within chromosomes that could potentially be expressed as visible metaphase chromosomal breakpoints. For instance, ionizing radiation deposits energy in the form of discrete radiation tracks (Goodhead 1992), which do not overlap at low doses. For high-linear energy transfer (LET) α-particle radiation, ionization events occur at high density along the whole length of the narrow track, but at a molecular level ionizations occur in 'clusters' and result in a non-random distribution of double strand breaks (dsb) of varying complexity (Goodhead 1991, Rydberg 1996). In addition, there is evidence to suggest that chromatin compaction, density of genes and distribution of transcription factors will influence chromosome exchange formation by making such sites either more prone to radiation-induced breakage and/or less likely to repair (Martinez-Lopez et al. 1998, Kiuru et al. 2000, Radulescu et al. 2004). Further, there is increasing evidence for functional associations between chromatin fibres from different chromosomes that have 'looped out' of their respective territories, suggesting preferential interactions between chromosomes could occur (Visser & Aten 1999, Volpi et al. 2000).

Numerous studies have been carried out to ascertain the role of chromatin structure and organization on the relative sensitivity of particular chromosomes and chromosome regions to different qualities of ionizing radiation. In the main these studies have employed both G-band and fluorescence *in situ* hybridization (FISH) techniques to identify chromosomal breakpoint positions for

Correspondence: R. M. Anderson, Cell and Chromosome Biology Group, Division of Biosciences, School of Health Sciences and Social Care, Brunel University, Uxbridge, West London UB8 3PH, UK. Tel: +44 (0)1895 267138. Fax: +44 (0)1895 274348. E-mail: rhona.anderson@brunel.ac.uk

ISSN 0955-3002 print/ISSN 1362-3095 online © 2006 Taylor & Francis
DOI: 10.1080/09553000600579231

individual chromosomes or for a selected group of chromosomes (for review see (Johnson et al. 1999)). Overall, a great deal of evidence has been generated that supports the non-random involvement of specific chromosomes in radiation-induced exchanges, but to date there remains limited consensus on which chromosomes these represent (Knehr et al. 1996, Barquinero et al. 1998, Cigarran et al. 1998, Scarpato et al. 2000). Equally, there are reports which predict a random distribution of chromosomal breakpoint position (Johnson et al. 1998, Cafourkova et al. 2001). Explanations for such contrasting reports between studies include differences in cell-type, radiation quality, dose, endpoint, scoring criteria and statistical methods used (Johnson et al. 1999).

On the question of statistical methodology, consideration for what is currently understood about the territorial organization of chromosomes in the nucleus can be accounted for by assuming chromosome territories to be spherical volumes (Cremer et al. 1996). However in addition to this, the dynamics of damaged chromatin (Savage 1993, Bornfleth et al. 1999, Figgitt & Savage 1999, Wu et al. 2001) and the cytogenetic method used for the detection of chromosome breaks, also require consideration. For example, the technique of multiplex-FISH (m-FISH) very efficiently detects inter-chromosomal rearrangements throughout the whole genome, but is a very poor system for detecting intra-chromosomal events. What this means is that breaks which have misrepaired as subtle intra-chromosome rearrangements will be unlikely to be included in any observed breakpoint distribution generated from m-FISH analysis. Therefore, whether a resolved fraction of chromosome breaks is best represented by statistical models based on either chromosome volume or chromosome surface area requires assumptions to be made as to where interchange repair events take place in the nucleus i.e., are interchanges only formed at chromosome territory boundary zones or can they also be formed within chromosome territories (Savage & Papworth 1973, Savage 2000, Cremer & Cremer 2001)?

For this contribution, we present chromosomal breakpoint distribution data collated from the damage induced in human peripheral blood lymphocytes (PBL) after exposure to a low dose of high-LET α-particles, corresponding to one α-particle traversal per cell. To our knowledge, these breakpoint distribution data represent the first produced by 24-colour karyotyping (m-FISH) where all chromosomes examined are differentially painted in the same hybridization experiment. The aims of this study are to assess the chromosomal break distribution observed in PBL 50 h after irradiation and identify 'hot'/'cold' α-particle-induced breakpoint spots by comparison with expected frequencies of chromosome break distributions based on either: (a) chromosome volume or (b) chromosome surface area. The data we present do show non-random involvement of specific chromosomes in the aberrations observed by m-FISH, despite the expectation that that the initial damage induced by each single high-LET α-particle is essentially random along the length of the α-particle track.

Materials and methods

Experimental methods

Chromosomal breakpoint assignation was carried out using a total of 167 damaged cells from a total of 934 cells analysed by m-FISH. This included 71 damaged cells from previously published data (Anderson et al. 2002) and 96 damaged cells from new unpublished data of α-particle-induced damage in human peripheral blood lymphocytes (PBL). In total, data from four different female donors was pooled for analysis. No statistical differences in aberration complexity or frequency of chromosome breaks were observed between any of these donors.

Cell culture and irradiation. Whole blood was collected from healthy volunteers according to the guidelines issued by the Medical Research Council in *Responsibility in Investigations on Human Participants and Material and on Personal Information* (MRC Ethics series, November 1992) and separated to isolate the PBL fraction using vacutainer-CPT mononuclear cell preparation tubes (BD Sciences, Cowley, Oxford, UK). Washed PBL were then plated as a monolayer and irradiated in G_0 with 0.5 Gy ^{238}Pu α-particles (3.26 MeV) (LET 121.4 keV/μm) (delivers on average of 1 α-particle per PBL). After irradiation, PBL were seeded at a density of 4×10^5 cells/ml in 4 ml volumes of growth media (Roswell Park Memorial Institute (RPMI) 1640 (Dutch modification; Gibco, Paisley, UK) containing 15% heat inactivated foetal bovine serum (FBS) (Gibco, Paisley, UK), 100 μg/ml streptomycin, 100 IU/ml penicillin, 2 mM L-glutamine, 2 mM sodium pyruvate (Sigma, Poole, UK), 12.5 μg/ml 5'-bromodeoxyuridine (BrdU) (Sigma, Poole, UK)) and stimulated to divide by the addition of 0.5 μg/ml purified phytohaemaglutinin (PHA: HA16) (Murex Biotech (UK) Ltd., Dartford, UK). PBL were subsequently harvested to obtain 1st division metaphase cells using standard cytogenetic techniques after 48 – 50 h in culture (Anderson et al. 2000).

Multiplex fluorescence in situ hybridization (m-FISH). Fresh slides of metaphase cells were hardened (3:1 methanol:acetic acid for 1 h, dehydrated through an ethanol series (2 min each in 70%, 70%, 90%, 90%

and 100%), baked at 65°C for 20 min, then 10 min in acetone) and pretreated with RNase A (Sigma, Poole, UK) (100 μg/ml in 2 × SSC) at 37°C for 1 h. After washing in 2 × (sodium salt citrate) SSC and phosphate buffered solution (PBS), the cells were treated with pepsin (Sigma, Poole, UK) ($1{:}20 \times 10^3$ in 10 mM HCL) at 37°C for 5 – 10 min then washed twice in PBS, 50 mM $MgCl_2$/PBS, 50 mM $MgCl_2$/1% formaldehyde/PBS then PBS before finally dehydrating through an ethanol series (2 min each in 70%, 70%, 90%, 90% and 100%). For hybridization, cells were denatured in 70% formamide/2 × SSC at 72°C for 3 min and dehydrated for 1 min each in 70/90/100% ethanol. In parallel, an aliquot of SpectraVision™ Assay (Vysis, Maidenhead, UK) 24-colour paint cocktail was denatured at 73°C for 6 min. Cells and probe were then mixed and left to hybridise for 36 – 48 h at 37°C before being washed in 0.4 × SSC/0.3% Igepal (Sigma, Poole UK) at 71°C for 2 – 3 min and in 2 × SSC/0.1% Igepal at room temperature for 10 sec. Cells were counterstained using 4′,6-diamidino-2-phenylindole (DAPI III) (Vysis, Maidenhead, UK), sealed and stored in the dark at −20°C.

m-FISH analysis. Chromosome aberrations were analysed as previously described (Anderson et al. 2003). In brief, metaphase chromosomes were visualized using a 6-position Olympus BX51 fluorescent microscope containing individual filter sets for each component fluor of the SpectraVision (Vysis, Maidenhead, (UK) Ltd) probe cocktail plus DAPI. Digital images were captured for m-FISH using a charged-coupled device (CCD) camera (Photometrics Sensys CCD) coupled to and driven by Genus (Applied Imaging, Newcastle, UK). In the first instance, cells were karyotyped and analysed by enhanced DAPI banding. Detailed paint analysis was then performed by assessing paint coverage for each individual fluor down the length of each individual chromosome, using both the raw and processed images for each fluor channel. A cell was classified as being apparently normal if all 46 chromosomes were observed by this process, and subsequently confirmed by the Genus m-FISH assignment, to have their appropriate combinatorial paint composition down their entire length. Abnormalities were identified as colour-junctions down the length of individual chromosomes and/or by the presence of chromosome fragments. The paint composition was used to identify the chromosomes involved. The assignment of a breakpoint to a specific chromosomal region (pter, p, peri-centromere, q or qter) was based on the DAPI banding pattern at the m-FISH colour junction, centromere location and size of the painted material on each rearranged chromosome. A detailed assignment of breakpoints to chromosome bands was not possible due to limits in DAPI resolution and no attempt was made to consider intra-chromosomal events such as inversions in this assessment.

Exchange aberrations involving 3 or more breaks in 2 or more chromosomes were classed as Complex and assigned the most conservative C/A/B (minimum number of Chromosomes/Arms/Breaks involved) (Savage & Simpson 1994), while exchange aberrations involving only two breaks in one or two chromosomes were classified as Simple. Chromosome breaks not involving additional chromosomes were classed as Break-only.

Statistical analysis

The relative position of each breakpoint on each damaged chromosome was determined as described above and assigned into 1 of 5 distinct sub-regions representing pter, p, peri-centromeric, q and qter. For comparative statistics to be performed it was necessary to define the relative lengths of each of these chromosomal sub-regions. This was achieved using a standard ideogram, marking specific G-band positions as region boundaries on each chromosome and directly measuring the length of each region. 'Measured' lengths were then converted, as proportions of the total chromosome length, into Morton's scale of physical chromosome length (Table I)

Table I. Relative length of chromosome regions pter, p, cen, q, qter.

	pter	p	cen	q	qter	Total		Pter	p	cen	q	qter	Total
1	19.2	89.6	38.4	96.6	19.2	263	12	12.6	15.9	21.0	80.9	12.6	143
2	19.6	59.8	39.2	116.8	19.6	255	13	2.2	5.2	17.2	76.5	12.9	114
3	18.2	62.7	36.3	78.7	18.2	214	14	2.2	5.1	17.4	71.2	13.1	109
4	16.1	23.8	32.2	114.8	16.1	203	15	2.2	6.2	17.3	67.4	13.0	106
5	16.2	23.7	24.2	113.7	16.2	194	16	10.4	18.1	20.9	38.1	10.4	98
6	11.9	41.1	23.9	94.1	11.9	183	17	10.2	7.6	20.4	43.6	10.2	92
7	12.1	40.9	24.1	81.9	12.1	171	18	10.1	1.8	16.2	46.8	10.1	85
8	12.4	27.3	20.7	82.3	12.4	155	19	9.1	13.7	14.5	20.7	9.1	67
9	12.1	28.8	20.1	71.8	12.1	145	20	10.6	11.9	16.9	21.9	10.6	72
10	12.0	22.0	20.0	78.0	12.0	144	21	2.2	3.4	10.9	22.7	10.9	50
11	12.0	36.0	20.0	64.0	12.0	144	22	2.2	5.2	11.2	26.2	11.2	56
X	12.6	36.8	25.2	76.8	12.6	164							

(Morton 1991). Thus, the relative length of the p-and q-arms varies for each chromosome and the terminal regions are proportionate to the total length of each chromosome.

To test for a non-random distribution of breaks between chromosomes, the observed numbers of breaks in each chromosome were compared with the corresponding expected numbers, the latter being calculated on the assumption that the distribution of breaks is random with regard to either chromosome volume (proportional to length) or surface area (proportional to length$^{2/3}$) (Cremer et al. 1996). Overall differences between observed and expected frequencies were compared using the Pearson chi-square test; exact significance levels were estimated by Monte Carlo simulation (Tarone 1989).

Observed and expected numbers of breaks in individual chromosomes were compared using the binomial test (De Braekeleer & Smith 1988). Chromosomes with significantly more breaks than expected ('hotspots') were identified by an upper-tail binomial test, those with significantly fewer breaks than expected ('coldspots') were identified by a lower-tail binomial test. However, the large number of comparisons involved (23 chromosomes) increases the risk that, even when the distribution of breaks is random, one or more chromosomes will be identified by this test as a hotspot or coldspot just by chance alone. The significance level used in the binomial test was therefore not the customary 0.05 but some level (ζ), smaller than 0.05, chosen so as to reduce the risk of obtaining one or more hot-(cold)spot by chance alone (the 'experimentwise false positive rate') to around 5%. This significance level ζ (which is different for the upper- and lower-tail tests) was estimated by Monte Carlo simulation (Tarone 1989). A chromosome was only identified as a hot-(cold)spot if the p-value in the binomal test was smaller than ζ.

The above tests, which were used to look for non-random distributions of breaks between chromosomes, were also used to test for a non-random distribution of breaks between the 5 regions (pter, p, cen, q, qter) within each chromosome, and to test whether any one of these 5 regions could be identified as a hot-(cold)spot.

Likewise, the same statistical analyses were used to test for a non-random distribution of breaks over the entire genome of 23 chromosomes $\times$ 5 regions, and to identify hot-(cold)spots among these 115 regions.

Results

The distribution of chromosome breaks observed by m-FISH after exposure to a mean of 1 high-LET α-particle per cell, were used to identify chromosomes and regions of chromosomes representative of breakpoint 'hot' ('cold') spots in human peripheral blood lymphocytes (PBL). Data from cells that contained damage to homologous chromosome pairs were excluded from this analysis in an effort to minimize mis-classification of breakpoint assignation.

Distribution of α-particle-induced breaks genome-wide

The observed distribution of breaks between whole chromosomes genome-wide is shown in comparison to the expected distribution of breaks based on either the volume of individual chromosomes (proportional to chromosome length) (Figure 1) or the surface area of individual chromosomes (proportional to chromosome length$^{2/3}$) (Figure 2). Overall, although there was a good general trend between observed and expected, a deviation from randomness was observed (Figures 1 and 2). This deviation was more apparent when the observed data were compared against the model of chromosome surface area rather than

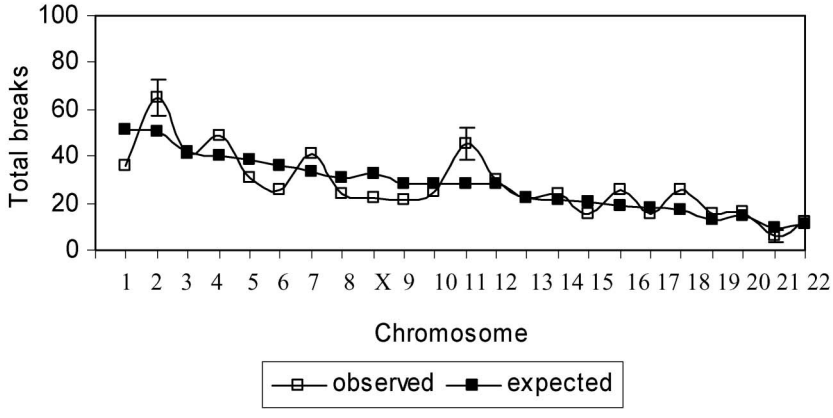

Figure 1. Distribution of chromosome breaks according to chromosome volume. Cells with damaged homologues excluded. Chi-square = 46.13; d.f. = 22; exact $p = 0.0020$. Lines between values are drawn as a visual aid. Standard errors are shown for the largest and smallest value, and for chromosome 11.

against chromosome volume (chi-square = 46.13; $p = 0.0020$ versus chi-square = 52.86; $p = 0.0005$) (Figures 1 and 2).

Table II details the data illustrated in Figures 1 and 2 and shows the significance levels for the individual chromosome comparisons (p-values). The significance level required to reduce the experiment-wise false positive rate to ~5% (see methods) is also shown (ζ). Using this adjusted level of significance, the number of breaks in chromosome 2 was over-represented compared to that expected based on the surface area of chromosome 2 ($p = 0.00034$) and chromosome 11 was over-represented according to both chromosome volume ($p = 0.0017$) and surface area ($p = 0.0022$). A detailed assessment of the break distribution within both chromosomes 2 and 11 was carried out but no particular region (pter, p, cen, q qter) was identified as containing more breaks than expected (data not shown).

Distribution of breaks in α-particle-induced complex exchanges

Complex aberrations are characteristically induced in PBL after exposure to high-LET α-particle radiation (Anderson et al. 2002). We therefore

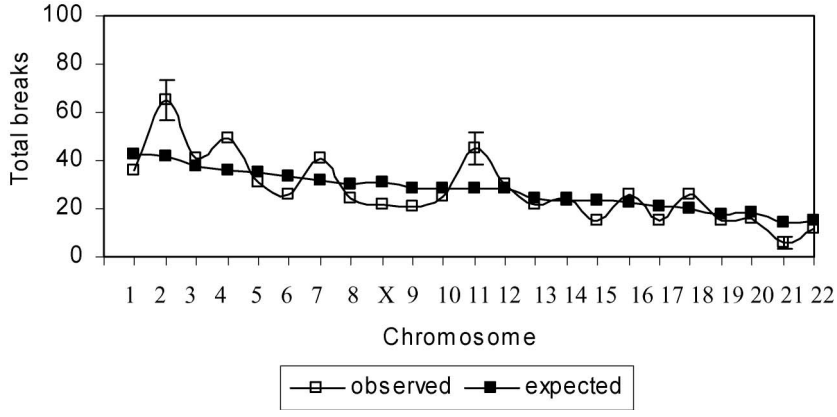

Figure 2. Distribution of chromosome breaks according to chromosome surface area. Cells with damaged homologues excluded. Chi-square = 52.86; d.f. = 22; exact $p = 0.0005$. Lines between values are drawn as a visual aid. Standard errors are shown for the largest and smallest value, and for chromosome 11.

Table II. Distribution of all breaks between chromosomes.

			Chromosome length			Chromosome length$^{2/3}$		
Chromosome	Length	Observed	Expected	p-value	ζ	Expected	p-value	ζ
1	263	36	52	0.011	0.0030	43	0.17	0.0032
2	255	65	50	0.019	0.0028	42	0.00034†	0.0026
3	214	41	42	0.48	0.0030	37	0.28	0.0026
4	203	49	40	0.081	0.0028	36	0.019	0.0026
5	194	31	38	0.14	0.0030	35	0.29	0.0032
6	183	26	36	0.048	0.0030	34	0.10	0.0032
7	171	41	34	0.11	0.0028	32	0.067	0.0026
8	155	24	30	0.13	0.0030	30	0.15	0.0032
9	145	21	28	0.087	0.0030	29	0.080	0.0032
10	144	25	28	0.31	0.0030	29	0.28	0.0032
11	144	45	28	0.0017†	0.0028	29	0.0022†	0.0026
12	143	30	28	0.38	0.0028	28	0.41	0.0026
13	114	22	22	0.53	0.0030	24	0.35	0.0032
14	109	24	21	0.31	0.0028	24	0.51	0.0026
15	106	15	21	0.12	0.0030	23	0.043	0.0032
16	98	26	19	0.078	0.0028	22	0.23	0.0026
17	92	15	18	0.28	0.0030	21	0.10	0.0032
18	85	26	17	0.019	0.0028	20	0.11	0.0026
19	67	15	13	0.34	0.0028	17	0.35	0.0032
20	72	16	14	0.34	0.0028	18	0.37	0.0032
21	50	6	10	0.14	0.0030	14	0.013	0.0032
22	56	12	11	0.42	0.0028	15	0.25	0.0032
X	164	22	32	0.035	0.0030	31	0.050	0.0032

ζ is the significance level required to reduce the experimentwise false positive rate to ~5% (see text). A chromosome is only regarded as a hotspot/coldspot if the p-value is less than ζ; such p-values are identified with †.

separated these aberrations to assess for any notable differences in breakpoint distribution to that which was observed genome-wide (Table III). Overall no differences were seen (Tables II and III). The number of breaks was over-represented in chromosome 2 according to chromosome surface area ($p = 0.00024$) and in chromosome 11 according to both chromosomal volume ($p = 0.0012$) and surface area ($p = 0.0015$). Again no particular region (pter, p, cen, q qter) of chromosome 2 or chromosome 11 was identified as containing more breaks than expected.

Distribution of α-particle-induced breaks not involved in an exchange

At the resolution of m-FISH and considering classification where free-ends are accounted for, chromosome 'break-only' appear to represent true-incomplete exchanges (Wu et al. 1999, Anderson et al. 2002). Thus to determine whether certain regions of the genome preferentially fail to rejoin, the distribution of breaks observed over the entire genome ($23 \times$ chromosomes 5 regions) was compared with the expected distribution based on the volume of each individual chromosome region. No significant departure from randomness was observed (chi-square $= 116.09$; d.f. $= 114$; exact $p = 0.41$). Nevertheless, when adjusted to account for false-positives, the long-arms of chromosomes 11 and 13 were identified as being over-represented ($p = 0.022$ and $p = 0.048$ respectively) (Table IV).

Distribution of α-particle-induced breaks in centromeric and telomeric regions

To test whether the repetitive elements in centromeric and telomeric regions were preferentially involved in chromosomal rearrangements, the distribution of breaks between each region, aggregated for all chromosomes, was compared with that which would be expected based on 'region' volume or 'region' surface area (Table V).

The chromosome regions identified as 'hot-(cold)-spots' varied depending on which model the expected frequencies of breaks were derived from. Specifically, for all breaks genome-wide, the p-arms and q-arms were identified as cold-spots and the centromere regions as a hot-spot when compared according to chromosome volume. This changed to p-ters and p-arms being cold-spots and the q-arms being a hot-spot, when the surface area of those regions were considered. Similarly, for break distribution in complex aberrations, the q-arms were cold-spots and the centromere region a hot-spot when compared according to volume, but when analysed according to

Table III. Distribution of breaks between chromosomes in α-particle-induced complexes.

			Chromosome length			Chromosome length$^{2/3}$		
Chromosome	Length	Observed	Expected	*p*-value	ζ	Expected	*p*-value	ζ
1	263	29	42	0.017	0.0030	35	0.17	0.0032
2	255	56	41	0.011	0.0026	34	0.0002†	0.0027
3	214	32	34	0.38	0.0030	30	0.41	0.0027
4	203	43	33	0.041	0.0026	29	0.009	0.0027
5	194	26	31	0.20	0.0030	29	0.36	0.0032
6	183	23	29	0.13	0.0030	27	0.22	0.0032
7	171	31	27	0.27	0.0026	26	0.19	0.0027
8	155	22	25	0.32	0.0030	24	0.34	0.0032
9	145	15	23	0.043	0.0030	23	0.039	0.0032
10	144	20	23	0.30	0.0030	23	0.28	0.0032
11	144	39	23	0.0012†	0.0026	23	0.0015†	0.0027
12	143	24	23	0.44	0.0026	23	0.47	0.0027
13	114	16	18	0.35	0.0030	20	0.22	0.0032
14	109	19	17	0.39	0.0026	19	0.52	0.0032
15	106	12	17	0.13	0.0030	19	0.056	0.0032
16	98	20	16	0.17	0.0026	18	0.36	0.0027
17	92	11	15	0.20	0.0030	17	0.07	0.0032
18	85	23	14	0.012	0.0026	16	0.07	0.0027
19	67	13	11	0.28	0.0026	14	0.46	0.0032
20	72	11	12	0.51	0.0030	15	0.20	0.0032
21	50	5	8	0.19	0.0030	12	0.026	0.0032
22	56	10	9	0.41	0.0026	12	0.30	0.0032
X	164	18	26	0.053	0.0030	26	0.072	0.0032

ζ is the significance level required to reduce the experimentwise false positive rate to ~5% (see text). A chromosome is only regarded as a hotspot/coldspot if the *p*-value is less than ζ; such p-values are identified with †.

Table IV. Distribution of chromosome breaks not involved in an exchange.

	pter		p		cen		q		qter	
C	E	O	E	O	E	O	E	O	E	O
1	0.21	0	0.97	0	0.42	2	1.05	0	0.21	0
2	0.21	0	0.65	1	0.43	2	1.27	0	0.21	0
3	0.20	0	0.68	3	0.39	0	0.85	2	0.20	0
4	0.17	0	0.26	0	0.35	0	1.25	1	0.17	0
5	0.18	0	0.26	0	0.26	0	1.23	1	0.18	0
6	0.13	0	0.45	1	0.26	0	1.02	0	0.13	0
7	0.13	0	0.44	0	0.26	2	0.89	1	0.13	0
8	0.13	0	0.30	0	0.22	0	0.89	0	0.13	0
9	0.13	0	0.31	0	0.22	0	0.78	1	0.13	0
10	0.13	0	0.24	1	0.22	1	0.85	2	0.13	0
11	0.13	0	0.39	0	0.22	1	0.69	5	0.13	0
12	0.14	0	0.17	0	0.23	0	0.88	1	0.14	0
13	0.02	0	0.06	0	0.19	0	0.83	5	0.14	0
14	0.02	0	0.06	0	0.19	0	0.77	0	0.14	0
15	0.02	0	0.07	0	0.19	0	0.73	0	0.14	0
16	0.11	0	0.20	0	0.23	1	0.41	0	0.11	0
17	0.11	0	0.08	0	0.22	0	0.47	0	0.11	0
18	0.11	0	0.02	0	0.18	0	0.51	0	0.11	0
19	0.10	0	0.15	0	0.16	0	0.22	0	0.10	0
20	0.11	0	0.13	0	0.18	0	0.24	0	0.11	0
21	0.02	0	0.04	0	0.12	0	0.25	0	0.12	0
22	0.02	0	0.06	0	0.12	0	0.28	0	0.12	0
X	0.14	0	0.40	0	0.27	0	0.83	1	0.14	0

C: chromosome, E: expected according to volume of individual chromosome region, O: number of breaks observed in that region not involved in a chromosome exchange.

Table V. Distribution of chromosome breaks between regions aggregated for all chromosomes.

			Chromosome length			Chromosome length$^{2/3}$		
	Chromosome region	Observed	Expected	*p*-value	ζ	Expected	*p*-value	ζ
Genome-wide	pter	53	49	0.28	0.012	70	0.014‡	0.011
	p	93	115	0.012‡	0.012	119	0.0036‡	0.011
	cen	132	100	0.0004†	0.012	116	0.059	0.011
	q	281	311	0.0095‡	0.012	245	0.0021†	0.011
	qter	74	59	0.023	0.012	82	0.19	0.011
Complex aberrations	pter	48	40	0.11	0.011	58	0.10	0.011
	p	76	94	0.02	0.011	98	0.0075‡	0.011
	cen	105	82	0.0036†	0.011	95	0.14	0.011
	q	227	254	0.0088‡	0.011	201	0.01†	0.011
	qter	62	48	0.023	0.011	67	0.28	0.011

ζ is the significance level required to reduce the experimentwise false positive rate to $\sim$5% (see text). A chromosome region is only regarded as a hotspot (†)/coldspot (‡) if the *p*-value is less than ζ.

surface area, the p-arms were identified as cold-spots and q-arms became hot-spots (Table V). When individual chromosomes were considered, this trend of p-arms being less involved and q-arms more involved than expected, according to their surface area, was maintained (data not shown).

Discussion

To test whether high-LET α-particle-induced damage in PBL is random at the cytogenetic level, the distribution of the relative breakpoint positions identified by m-FISH were compared with the distribution that would be expected if the breaks occurred randomly. Expected break frequencies were calculated according to either the volume (proportional to chromosome length) or the surface area (proportional to chromosome length$^{2/3}$) of individual chromosomes or regions of chromosomes. Overall, deviations from randomness were observed (Figures 1 and 2) and the degree of this deviation varied depending on which statistical

model was used to calculate the expected frequencies.

An example that highlights this is shown by the distribution of breaks that were observed by m-FISH and assigned as occurring in one of the 5 chromosome regions (pter, p, cen, q, qter) (Table V). When compared according to chromosome length, the data show chromosome breaks to preferentially occur in centromeric regions, consistent with the suggestion that exchanges preferentially occur at repetitive sites (Chadwick & Leenhouts 1978, Natarajan et al. 1994, Surralles et al. 1997). However, this effect was lost when the same data were compared according to the surface area of each region, such that breaks were over-represented in the q-arms but under-represented in the p-arms (Table V). Assuming chromosome arms also form discrete spherical domains in interphase, this difference in break frequency between the chromosome arms could be a consequence of the q-arms having a smaller relative surface area:volume ratio compared to the p-arms. In other words, more breaks could be mis-repaired at the inter-chromosome boundaries and therefore be detected by m-FISH (accounting for more breaks in q-arm) than the intra-chromosome boundaries which, in the main, cannot be detected by m-FISH (accounting for less breaks in the p-arms). Following from this, repetitive non-transcribed sequences such as centromeric DNA, are not thought to arrange on the periphery of chromosome territories, possibly accounting for the observation that inter-changes in these regions are not over-represented according to surface area predictions (Mahy *et al.* 2002) (Table V). Overall, a statistical model that predicts break distribution based on the surface area of a chromosome territory is favoured (Wu et al. 2001, Cigarran et al. 2004). How 'convoluted' this surface area is and therefore what 'depth' or volume should also be considered for chromosome break distribution models (i.e., maximum migration distance for repair), remains to be established.

More breaks were observed on chromosome 11 and chromosomes 2 and 11 than would be expected based on their individual length or surface areas respectively. This observation was seen when all breaks genome-wide, or just those involved in complex aberrations, were considered (Tables II and III). There was no evidence to suggest chromosomes 2 and 11 were commonly involved in the same rearrangements. Within both chromosomes, breaks were randomly distributed and there was no evidence of any particular region (pter, p, cen, q, qter) dominating. Xiao and Natarajan (1999) similarly observed a higher than expected frequency of chromosome breaks in chromosome 8 in Chinese hamster embryonic cells after exposure to X-rays which they related to the occurrence of interstitial telomeric repeats throughout the length of this chromosome (Xiao & Natarajan 1999). Representative of ancestral fusions which are sensitive to radiation-induced and spontaneous breaks, these repeats are implicated in the formation of fragile sites (Boutouil et al. 1996). A number of known fragile sites in human cells have been identified on both chromosome 2 and chromosome 11, but it is unclear whether these sites confer any more sensitivity for breakage than those identified on similarly sized chromosomes (e.g., chromosome 1 or chromosome 12). A search of the literature reveals no evidence for the over-involvement of chromosome 2 in radiation-induced breaks, only an under-representation of chromosome 2 has been reported (Knehr et al. 1996, Braselmann et al. 2003, Cigarran et al. 2004). Further, there is no evidence for the over-involvement of either 11q or 13q in radiation-induced incomplete exchanges similar to those that were detected in this study. Interestingly though, chromosome 11 has recently been reported to be involved in more X-ray-induced breaks relative to its length (Cigarran et al. 2004). Chromosome 11 is gene-rich and involved in a vast array of different translocations recurrent in various leukaemia's, including secondary (radiation) therapy-related leukaemia's, while deletions of 11q and 13q are common in lymphoid neoplasia's (Dessen & Huret 2002).

In conclusion, a deviation from randomness in the distribution of high-LET α-particle-induced breaks in PBL was observed, and this was greatest when data was compared according to the relative surface area of each individual chromosome. Overall, there was no evidence to suggest that this non-randomness represented functional sites of pre-existing chromatin associations (Volpi et al. 2000). Within the resolution limits of this technique therefore, our data are inconsistent with the concept that α-particle-induced complex aberrations predominantly form though chance damage and repair within such sites. Instead, our data are in keeping with previous observations that if a chromosome territory is intersected by a high-LET α-particle then the likelihood of chromatin from that territory being 'hit' and subsequently resolved as damaged, is high (Goodwin et al. 1994, Anderson et al. 2002). Further, the concept that exchange aberrations are formed at boundary zones of chromosome territories and that their occurrence is dependent on common surface area, is supported (Savage & Papworth 1973, Cremer et al. 1996). Overall therefore at the cytogenetic level of m-FISH, the distribution of breaks induced by the nuclear traversal of a single high-LET α-particle is essentially random along the length of the particle track.

Acknowledgements

The authors would like to thank David Stevens and Mark Hill from the Biophysics Group, MRC Harwell for all α-particle irradiations. This work was supported by the Department of Health, UK (Grant RRX 95).

References

Anderson RM, Marsden SJ, Paice SJ, Bristow AE, Kadhim MA, Griffin CS, Goodhead DT. 2003. Transmissible and non-transmissible complex chromosome aberrations characterized by three-color and mFISH define a biomarker of exposure to high-LET alpha particles. Radiation Research 159:40–48.

Anderson RM, Marsden SJ, Wright EG, Kadhim MA, Goodhead DT, Griffin CS. 2000. Complex chromosome aberrations in peripheral blood lymphocytes as a potential biomarker of exposure to high-LET alpha-particles. International Journal of Radiation Biology 76:31–42.

Anderson RM, Stevens DL, Goodhead DT. 2002. M-FISH analysis shows that complex chromosome aberrations induced by alpha-particle tracks are cumulative products of localized rearrangements. Proceedings of the National Academy of Sciences of the United States of America 99:12167–12172.

Barquinero JF, Knehr S, Braselmann H, Figel M, Bauchinger M. 1998. DNA-proportional distribution of radiation-induced chromosome aberrations analysed by fluorescence in situ hybridization painting of all chromosomes of a human female karyotype. International Journal of Radiation Biology 74:315–323.

Bornfleth H, Edelmann P, Zink D, Cremer T, Cremer C. 1999. Quantitative motion analysis of subchromosomal foci in living cells using four-dimensional microscopy. Biophysics Journal 77:2871–2886.

Boutouil M, Fetni R, Qu J, Dallaire L, Richer CL, Lemieux N. 1996. Fragile site and interstitial telomere repeat sequences at the fusion point of a de novo (Y;13) translocation. Human Genetics 98:323–327.

Braselmann H, Kulka U, Huber R, Figel HM, Zitzelsberger H. 2003. Distribution of radiation-induced exchange aberrations in all human chromosomes. International Journal of Radiation Biology 79:393–403.

Cafourkova A, Lukasova E, Kozubek S, Kozubek M, Govorun RD, Koutna I, Bartova E, Skalnikova M, Jirsova P, Pasekova R, Krasavin EA. 2001. Exchange aberrations among 11 chromosomes of human lymphocytes induced by gamma-rays. International Journal of Radiation Biology 77:419–429.

Chadwick KH, Leenhouts HP. 1978. The rejoining of DNA double-strand breaks and a model for the formation of chromosomal rearrangements. International Journal of Radiation Biology Relat Stud Phys Chem Med 33:517–529.

Cigarran S, Barrios L, Barquinero JF, Caballin MR, Ribas M, Egozcue J. 1998. Relationship between the DNA content of human chromosomes and their involvement in radiation-induced structural aberrations, analysed by painting. International Journal of Radiation Biology 74:449–455.

Cigarran S, Barrios L, Caballin MR, Barquinero JF. 2004. Effect of DMSO on radiation-induced chromosome aberrations analysed by FISH. Cytogenetic and Genome Research 104:168–172.

Cremer C, Munkel C, Granzow M, Jauch A, Dietzel S, Eils R, Guan XY, Meltzer PS, Trent JM, Langowski J, Cremer T. 1996. Nuclear architecture and the induction of chromosomal aberrations. Mutation Research 366:97–116.

Cremer T, Cremer C. 2001. Chromosome territories, nuclear architecture and gene regulation in mammalian cells. Nature Reviews Genetics 2:292–301.

De Braekeleer M, Smith B. 1988. Two methods for measuring the non-randomness of chromosome abnormalities. Annals of Human Genetics 52(Pt 1):63–67.

Dessen P, Huret J. (2002) Chromosome 11 and Chromosome 13. Atlas of Genetic, Cytogenetic, Oncology and Haematology. URL: http://www.infobiogen.fr/services/chromcancer/indexbychromosome.

Figgitt M, Savage JRK. 1999. Interphase chromosome domain reorganization following irradiation. International Journal of Radiation Biology 75:811–817.

Goohead DT. 1991. Radiationtracks in biological materials: Initial damage in cells, DNA and associated structures. In Genes, Cancer and Radiation Protection, Edited by Mendelson ML. Published by NCRP. pp. 25–37.

Goodhead DT. 1992. Track structure considerations in low-dose and low-dose rate effects of ionizing-radiation. Advances in Radiation Biology 16:7–44.

Goodwin EH, Blakely EA, Tobias CA. 1994. Chromosomal damage and repair in G1-phase Chinese hamster ovary cells exposed to charged-particle beams. Radiation Research 138:343–351.

Johnson KL, Brenner DJ, Nath J, Tucker JD, Geard CR. 1999. Radiation-induced breakpoint misrejoining in human chromosomes: random or non-random? International Journal of Radiation Biology 75:131–141.

Johnson KL, Tucker JD, Nath J. 1998. Frequency, distribution and clonality of chromosome damage in human lymphocytes by multi-color FISH. Mutagenesis 13:217–227.

Kiuru A, Lindholm C, Auvinen A and Salomaa S. 2000. Localization of radiation-induced chromosomal breakpoints along human chromosome 1 using a combination of G-banding and FISH. International Journal of Radiation Biology 76: 667–672.

Knehr S, Zitzelsberger H, Braselmann H, Nahrstedt U, Bauchinger M. 1996. Chromosome analysis by fluorescence in situ hybridization: further indications for a non-DNA-proportional involvement of single chromosomes in radiation-induced structural aberrations. International Journal of Radiation Biology 70:385–392.

Mahy NL, Perry PE, Bickmore WA. 2002. Gene density and transcription influence the localization of chromatin outside of chromosome territories detectable by FISH. Journal of Cell Biology 159:753–763.

Martinez-Lopez W, Boccardo EM, Folle GA, Porro V, Obe G. 1998. Intrachromosomal localization of aberration breakpoints induced by neutrons and gamma rays in Chinese hamster ovary cells. Radiation Research 150:585–592.

Morton NE. 1991. Parameters of the human genome. Proceedings of the National Academy of Sciences of the United States of America 88:7474–7476.

Natarajan AT, Balajee AS, Boei JJ, Chatterjee S, Darroudi F, Grigorova M, Noditi M, Oh HJ, Slijepcevic P, Vermeulen S. 1994. Recent developments in the assessment of chromosomal damage. Intternational Journal of Radiation Biology 66:615–623.

Radulescu I, Elmroth K, Stenerlow B. 2004. Chromatin organization contributes to non-randomly distributed double-strand breaks after exposure to high-LET radiation. Radiation Research 161:1–8.

Rydberg B. 1996. Clusters of DNA damage induced by ionizing radiation: formation of short DNA fragments. II. Experimental detection. Radiation Research 145:200–209.

Savage JR. 2000. Cancer. Proximity matters. Science 290:62–63.

Savage JR. 1993. Interchange and intra-nuclear architecture. Environ Mol Mutagen 22:234–244.

Savage JR, Papworth DG. 1973. The relationship of radiation-induced dicentric yield to chromosome arm number. Mutation Research 19:139–143.

Savage JR, Simpson PJ. 1994. FISH 'painting' patterns resulting from complex exchanges. Mutation Research 312:51–60.

Scarpato R, Lori D, Tomei A, Cipollini M, Barale R. 2000. High prevalence of chromosome 10 rearrangements in human lymphocytes after in vitro X-ray irradiation. International Journal of Radiation Biology 76:661–666.

Surralles J, Darroudi F, Natarajan AT. 1997. Low level of DNA repair in human chromosome 1 heterochromatin. Genes Chromosomes and Cancer 20:173–184.

Tarone RE 1989. Testing for non-randomness of events in sparse data situations. Annals of Human Genetics 53(Pt 4):381–387.

Visser AE, Aten JA. 1999. Chromosomes as well as chromosomal subdomains constitute distinct units in interphase nuclei. Journal of Cell Science 112(Pt 19):3353–3360.

Volpi EV, Chevret E, Jones T, Vatcheva R, Williamson J, Beck S, Campbell RD, Goldsworthy M, Powis SH, Ragoussis J, Trowsdale J, Sheer D. 2000. Large-scale chromatin organization of the major histocompatibility complex and other regions of human chromosome 6 and its response to interferon in interphase nuclei. Journal of Cell Science 113(Pt 9):1565–1576.

Wu H, Durante M, Lucas JN. 2001. Relationship between radiation-induced aberrations in individual chromosomes and their DNA content: effects of interaction distance. International Journal of Radiation Biology 77:781–786.

Wu H, George K, Yang TC. 1999. Estimate of the frequency of true incomplete exchanges in human lymphocytes exposed to 1 GeV/u Fe ions in vitro. International Journal of Radiation Biology 75:593–599.

Xiao Y, Natarajan AT. 1999. Non-proportional involvement of Chinese hamster chromosomes 3, 4, 8 and 9 in X-ray-induced chromosomal aberrations. International Journal of Radiation Biology 75:943–951.